Structural, magnetic, Mössbauer and magnetostrictive studies of amorphous $Tb(Fe_{0.55}Co_{0.45})_{1.5}$ films

2000 J. Phys.: Condens. Matter 12 8283

(http://iopscience.iop.org/0953-8984/12/38/305)

J. Phys.: Condens. Matter **12** (2000) 8283–8293. Printed in the UK PII: S0953-8984(00)15123-9

Structural, magnetic, Mössbauer and magnetostrictive studies of amorphous $Tb(Fe_{0.55}Co_{0.45})_{1.5}$ films

N H Duc†‖, T M Danh†, H N Thanh†, J Teillet‡ and A Liénard§

† Cryogenic Laboratory, Faculty of Physics, National University of Hanoi, 334 Nguyen Trai, Thanh Xuan, Hanoi, Vietnam
‡ Laboratoire de Magnétisme et Applications, GMP–UMR 6634, Université de Rouen, 76821 Mont-Saint-Aignan, France
§ Laboratoire de Magnétisme Louis Néel, CNRS, 38042 Grenoble Cedex 9, France

E-mail: duc@cryolab.edu.vn

Received 3 July 2000

Abstract. Films with a nominal composition of $Tb(Fe_{0.55}Co_{0.45})_{1.5}$ were fabricated by rf-magnetron sputtering from a fixed target configuration at various Ar gas pressures. Samples were investigated by means of x-ray diffraction (XRD), scanning electron microscopy (SEM), vibrating sample magnetometer (VSM), conversion electron Mössbauer spectra (CEMS) and magnetostriction measurements. As the Ar pressure increases, the Tb and Fe content increases slightly, whereas the Co content decreases. In addition, a small amount of Ar is introduced into the films. The as-deposited films are amorphous alloys, but their magnetic behaviour depends strongly on the deposition conditions: a perpendicular magnetic anisotropy is obtained only in film deposited at lowest Ar pressure and a parallel magnetic anisotropy exhibits in remaining films. These samples show an intrinsic magnetostriction ($\lambda \approx 10^{-3}$) in an applied field of 0.7 T. In this state, it was determined that the hyperfine field reaches the value $B_{hf} = 24.5$ T. Effects of the heat treatment on the magnetostrictive softness are also reported. The parallel magnetostriction with a huge magnetostrictive susceptibility ($\chi_\lambda = 1.8 \times 10^{-2}$ T^{-1}) obtained at ($\mu_0 H = 10$ mT) makes these materials useful for applications.

1. Introduction

Giant magnetostrictive materials in thin film form are very useful for microactuator devices [1–4]. For these applications, large low-field magnetostrictive susceptibilities, ($\chi_\lambda = \mathrm{d}\lambda_\parallel/\mathrm{d}(\mu_0 H) > 2 \times 10^{-2}$ T^{-1}), and low coercive fields ($\mu_0 H_C \ll 100$ mT), are required [5]. Research on these materials, thus, concentrates on reducing the necessary driving magnetic fields. Different approaches have been taken based on amorphous $(Tb, Dy)(Fe, Co)_2$ asperimagnets [6, 7]. In these alloys, the R–FeCo exchange energies are stronger than those in the 'pure' a-RFe and a-RCo alloys. This was thought to be the reason for the closing of the cone type distribution of (Tb, Dy) moments, then the enhancement of the R moment at room temperature and thus the magnetostriction. Recently, we have studied the magnetization and magnetostriction in the amorphous $(Tb, Dy)(Fe, Co)_{2.1}$ thin films [6, 7]. Indeed, a magnetostriction of 1020×10^{-6} was obtained in the applied field of 2 T for amorphous $Tb(Fe_{0.45}Co_{0.55})_{2.1}$ [6]. The optimization of magnetostriction and ordering temperature has been reported for TbDyFe/Nb multilayers by combining the advantages of a crystallized film

‖ Corresponding author.

0953-8984/00/388283+11$30.00

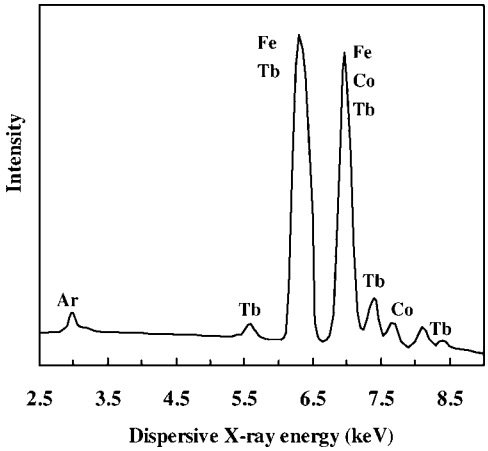

Figure 1. Dispersive x-ray energy for the $Tb(Fe_{0.55}Co_{0.45})_{1.5}$ film. The peak of Ar is obviously recognized.

(high T_C and giant λ) with soft magnetic properties of an amorphous phase [5]. In these materials, however, the coercive fields were raised ($\mu_0 H_C \approx 100$ mT). In principle, it is well known that the richer the rare-earth compound, the larger the spontaneous magnetostriction is. Thus, another optimization of room-temperature magnetostriction can also be obtained by combining the rare-earth composition and their ordering temperature. In view of this, the crystallized R–Fe alloys with the greatest potential to achieve large room temperature magnetostrictions are the cubic Laves phase RFe_2 compounds [8], whereas the amorphous ones are the $RFe_{1.5}$ alloys [9, 10]. In addition, it is also expected that similar effects of the substitution of Fe by Co on the enhancement of the magnetostriction found for 1:2 thin films would also be observed for this 1:1.5 amorphous phase [6, 11].

In this paper, we studied the structure, magnetization, Mössbauer spectra and magnetostriction of the amorphous films with a nominal composition of $Tb(Fe_{0.55}Co_{0.45})_{1.5}$ fabricated in different Ar gas pressures. Annealing effects make these films magnetically soft and, thus, useful for applications.

2. Experiment

The films with a nominal composition of $Tb(Fe_{0.55}Co_{0.45})_{1.5}$ were fabricated by rf-magnetron sputtering from a fixed target configuration at various Ar gas pressures. The typical power during sputtering was 400 W and the Ar gas pressure was around 10^{-2} mbar. A composite target consisted of 18 segments of about 20 degrees, of different elements (here Tb, Fe, Co). The substrates were glass microscope cover-slips with a nominal thickness of 150 μm. Both target and sample holder were water cooled. The thickness was measured mechanically using an α-step. The film thickness was ranging from 0.5 to 1.2 μm without any coating. The film composition was determined by energy-dispersive x-ray (EDX) (figure 1) and microstructure investigation (figure 2) was performed using a scanning electron microscope. The film structure was investigated by x-ray θ–2θ diffraction (XRD) with Cu Kα rays. The results showed the as-deposited samples to be amorphous (figure 3).

Samples were annealed at temperatures from 250 to 450 °C for 1 hour in a vacuum of 5×10^{-4} mbar in order to relieve any stress induced during the sputtering process. Subsequent

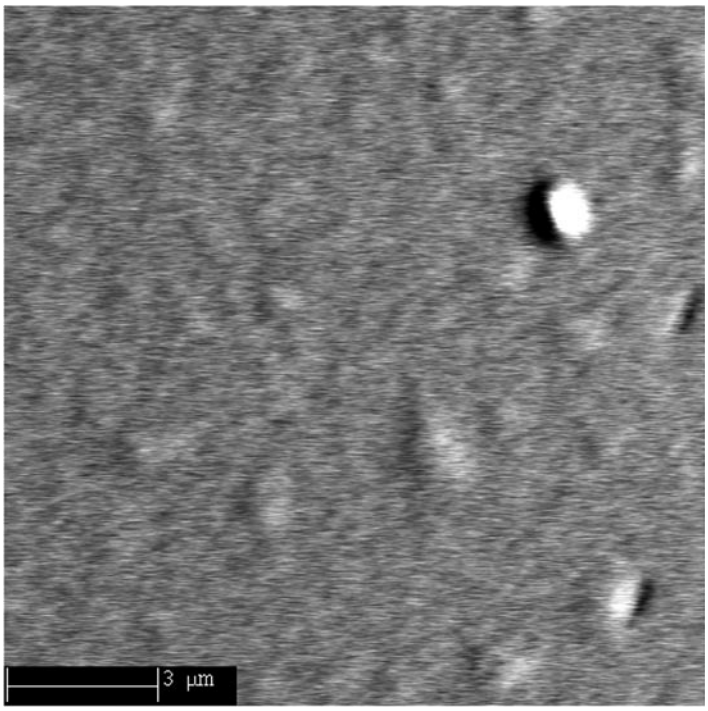

(a)

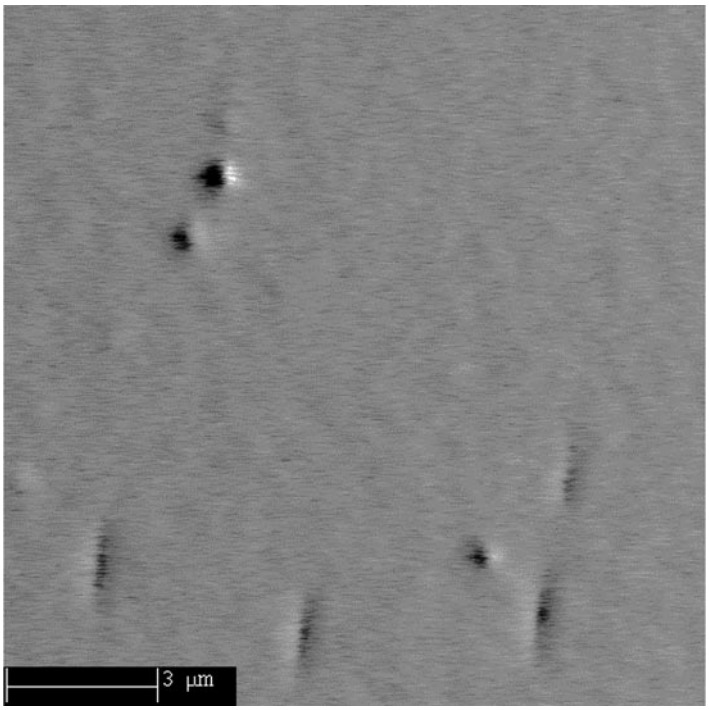

(b)

Figure 2. Micrograph for films A: (a) as-deposited and (b) annealed at 350 °C.

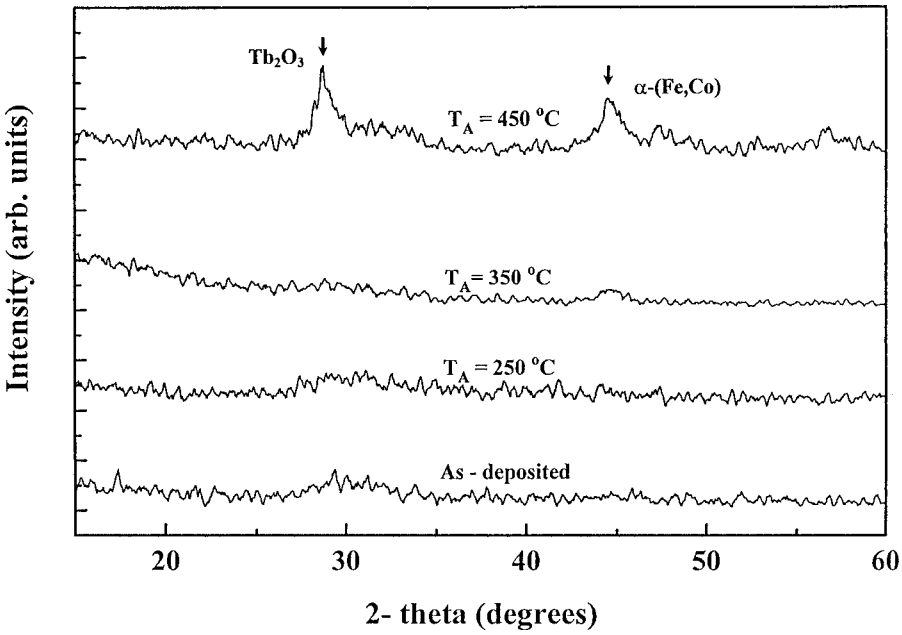

Figure 3. X-ray diffraction patterns of film A.

x-ray θ–2θ diffraction showed no evidence for a global crystallization after annealing, but the peaks of Tb oxides and α-(Fe, Co) appear due to the surface oxidation, see also figure 3.

The magnetization measurements were carried out using a vibrating sample magnetometer (VSM) in a field of up to 1.3 T at 300 K.

The conversion electron Mössbauer spectra (CEMSs) at room temperature were recorded using a conventional spectrometer equipped with a home-made helium-methane proportional counter. The source was ^{57}Co in a rhodium matrix. The films were set perpendicular to the incident γ-beam. The spectra were fitted with a least-squares technique using a histogram method relative to discrete distributions, constraining the line-widths of each elementary spectrum to be the same. Isomer shifts are given relative to α-Fe at 300 K. The average 'cone-angle' β between the incident γ-ray direction (being the direction normal to the film) and that of the hyperfine field B_{hf} (or the Fe magnetic moment direction) is estimated from the line-intensity ratios $3{:}x{:}1{:}1{:}x{:}3$ of the six Mössbauer lines, where x is related to β by $\sin^2\beta = 2x/(4+x)$.

The magnetostriction was measured using an optical deflectometer (resolution of 5×10^{-6} rad), in which the bending of the substrate due to the magnetostriction in the film was measured [12, 13].

3. Experimental results and discussion

Four samples, named A, B, C and D, were deposited from a fixed target configuration, but with different Ar gas pressures (ranging from 5 to 15 mbar, see table 1). The resulting thickness, composition and Ar contamination are summered in table 1. It can be seen from this table that as the Ar gas pressure increases, the deposition rate and the Co content decrease, whereas only a weak increase is observed for the Tb and Fe content. These composition variations can be understood by the difference in the scattering of sputtered Tb, Fe and Co particles [14].

Table 1. Sample characterization of Tb(Fe$_{0.55}$Co$_{0.45}$)$_{1.5}$ films.

Samples	Thickness (μm)	Ar gas pressure (mbar)	Deposition rate (nm min^{-1})	Tb content (%)	Fe content (%)	Co content (%)	Ar content (%)
A	1.15	5	3.5	40.4	32.0	27.0	0.6
B	0.7	8	3.1	40.6	32.2	26.4	0.8
C	0.5	10	2.7	40.8	32.6	25.6	1.0
D	0.6	15	2.4	41.2	32.6	25.0	1.2

Moreover, as indicated by the EDX results (figure 1), a small amount of Ar atoms is introduced into the films. This Ar content increases with increasing Ar gas pressure.

The magnetic hysteresis loops measured with applied magnetic field in the film-plane and film-normal directions are presented in figures 4 and 5 for the films A and D, respectively. It is clearly seen from these figures that magnetic properties of these films are rather different. The as-deposited film A exhibits a perpendicular anisotropy, whereas the films B, C and D show an in-plane anisotropy (see, e.g. figures 4(a) and 5(a)). Here, corrections with regard to the demagnetizing fields are not made, so the loops shown in the figures are more inclined than the 'true' ones. In [14], it was reported that the direction of the anisotropy depends mainly on the film composition, but it is nearly independent of the Ar gas pressure. In addition, the anisotropy change (from perpendicular to in-plane) can also be connected to the effects of sputtering condition [2, 9, 10]. At present, this argument seems to be the case because the Tb composition was observed to vary very little. As regards the magnetoelastic anisotropy, any magnetostrictive material always tries to compensate the external or internal stress by appropriate rotation of spins. For a film with positive magnetostriction, tensile stress leads to a spin orientation in the film plane whereas for compressive stress the spins orient along the film normal. The observed anisotropy change may imply that the sign and the magnitude of the film's stress were changed by the fabrication conditions.

The demagnetization process and the coercive field are also different in the as-deposited films under consideration. For the films C and D, the demagnetization shows a two-step-like process and a rather large coercivity ($\mu_0 H_C = 0.23$ T for film C and 0.34 T for film D). For film A, however, the two-step-like demagnetization disappears and $\mu_0 H_C$ is reduced (e.g. the film-normal coercivity, $\mu_0 H_{C\perp} = 0.132$ T and film-plane $\mu_0 H_{C\parallel} = 0.08$ T). While, intrinsically, related to the strong local anisotropy of the R atoms and their random distribution of easy axes present in such sperimagnetic systems, the demagnetization process and coercivity are strongly affected by internal stress, microstructure and homogeneity [14]. At present, the origin of the two-step-like demagnetization is still not clarified.

The CEMS is suitable to investigate hyperfine parameters of the iron nuclei within a depth range of about 200 nm from the film surface. Figure 6 presents the CEM spectra for the as-deposited films A, C and D. The spectra are typical of a distribution of iron environments and the slight asymmetry could be taken into account by a correlation between the isomer shift and the hyperfine field. However, due to the poor statistics, the spectra were fitted only with a distribution of hyperfine fields. The fine structure of the fitted spectra is probably due to least-squares fitting problems related to the poor statistics. Despite this less good statistics, the information about the average hyperfine field ($\langle B_{hf} \rangle$) and the Fe-spin reorientation ($\langle \beta \rangle$ angle) can be extracted from these spectra. The perpendicular anisotropy of the film A is characterized by the near disappearance of the second and fifth Mössbauer lines (figure 6(a)). For the films B and C, the in-plane anisotropy is evidenced by the enhancement of the second and fifth Mössbauer lines with respect to the remaining lines (figures 6(b) and (c)). The fit by

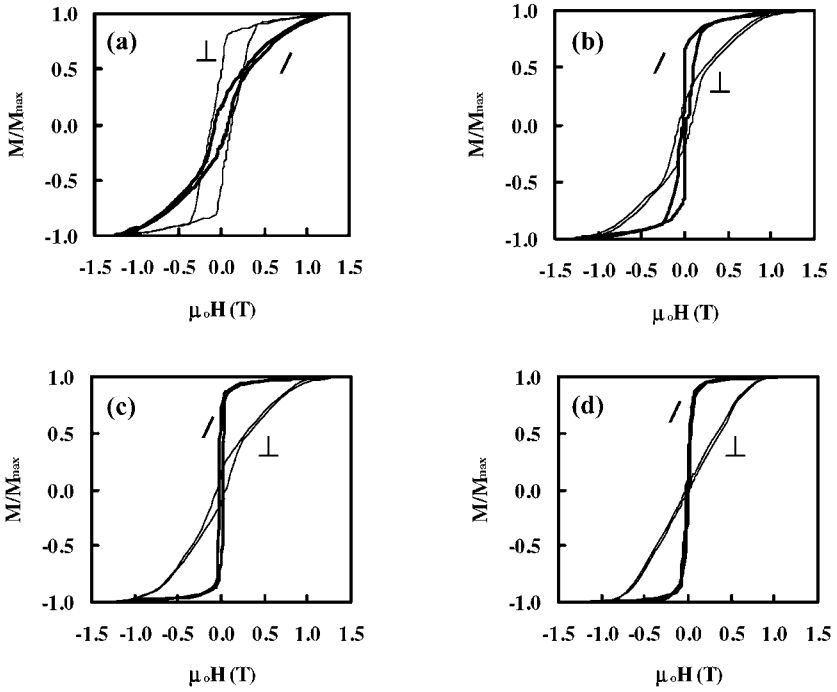

Figure 4. Magnetic hysteresis loops in the internal magnetic fields at 300 K for film A: (a) the as-deposited films, (b) after annealing at 250 °C, (c) 350 °C and (d) 450 °C.

the distribution of hyperfine field $P(B_{hf})$ provides an average value of $\langle B_{hf}\rangle = 23.5$ T and $\langle\beta\rangle = 12$ degrees for film A and of $\langle B_{hf}\rangle = 24.5$ T and $\langle\beta\rangle = 76$ degrees for films D and C. The $\langle B_{hf}\rangle$ values obtained for these amorphous $Tb(Fe_{0.55}Co_{0.45})_{1.5}$ phases are somewhat larger than that of 21 T reported for the amorphous $TbFe_2$ alloy [17]. Such a result implies stronger 3d–3d exchange interactions. The 3d magnetic moment (M_{3d}) is determined by scaling with $\langle B_{hf}\rangle$, taking $\langle B_{hf}\rangle = 33.4$ T and $M_{3d} = 2.2\ \mu_B$/at for α-Fe. This results in $M_{3d} \approx 1.6\,\mu_B$/at. This finding is in good agreement with that deduced from magnetization data for a-(Tb, Dy)(Fe, Co)$_2$ films [7]. This large room-temperature 3d magnetic moment indicates that in the composition under consideration, although the Tb composition is rich, there was sufficient Co to ensure good ferromagnetic T–T coupling as well as sufficient Fe giving the large 3d magnetic moment.

The heat treatment causes a number of clear differences in the magnetization process. Firstly, the magnetic anisotropy changes from perpendicular to parallel (see figures 4(a)–(d)). Secondly, the coercive field is strongly reduced: for instance, with the annealing at $T_A = 450$ °C, $\mu_0 H_{C\parallel}$ is equal to 6 mT. Thirdly, the saturation magnetization decreases, but can be easily reached at low magnetic fields. In agreement with the XRD results, the reduction of the magnetization may relate to the process of oxidation during vacuum heat treatment. This effect was previously reported by Wada *et al* [18]. The annealing effects on the improvement of the magnetic softness are considered to be the best for the film D annealed at $T_A = 350$ °C: a typical hysteresis loop with $\mu_0 H_C$ of below 5 mT and saturating at 25 mT, see figure 5(c). The elimination of the coercivity and anisotropy with annealing reflects that an isotropic amorphous structure has lower energy than the as-deposited anisotropy state. The relaxation of the anisotropy without crystallization, thus, is a simple relaxation of the amorphous structure resulting in a more stable and homogenous film structure, see also the micrograph in figure 2(b).

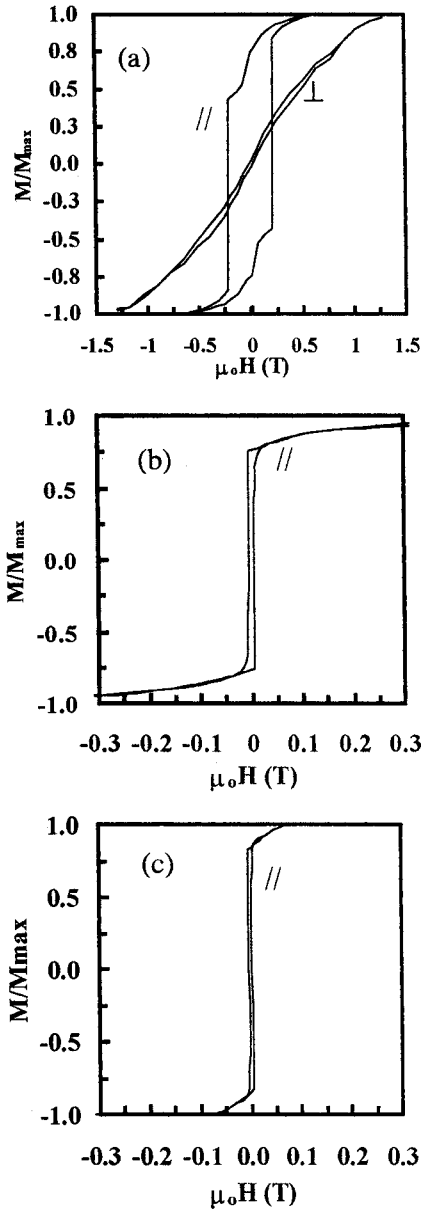

Figure 5. Magnetic hysteresis loops in the internal magnetic fields at 300 K for film D: (a) the as-deposited films, (b) after annealing at 250 °C and (c) 350 °C.

The CEMS spectra was also recorded and fitted with a wide distribution of hyperfine fields for the film A annealed at $T_A = 450\,^{\circ}$C. For this sample, the peak at 23.5 T, which corresponds to the magnetostrictive Tb–FeCo phase still exists in the $P(B_{hf})$ curve; however, it was weakened and broadened. Moreover, the high-hyperfine-field contribution becomes dominant. A sharp $P(B_{hf})$-peak is reached at 34.5 T. In accordance with the XRD results, this major ferromagnetic component (82% of the total spectrum area) is associated with the contribution of the crystallized α-(Fe, Co) phase formed at the film surface due to the oxidation.

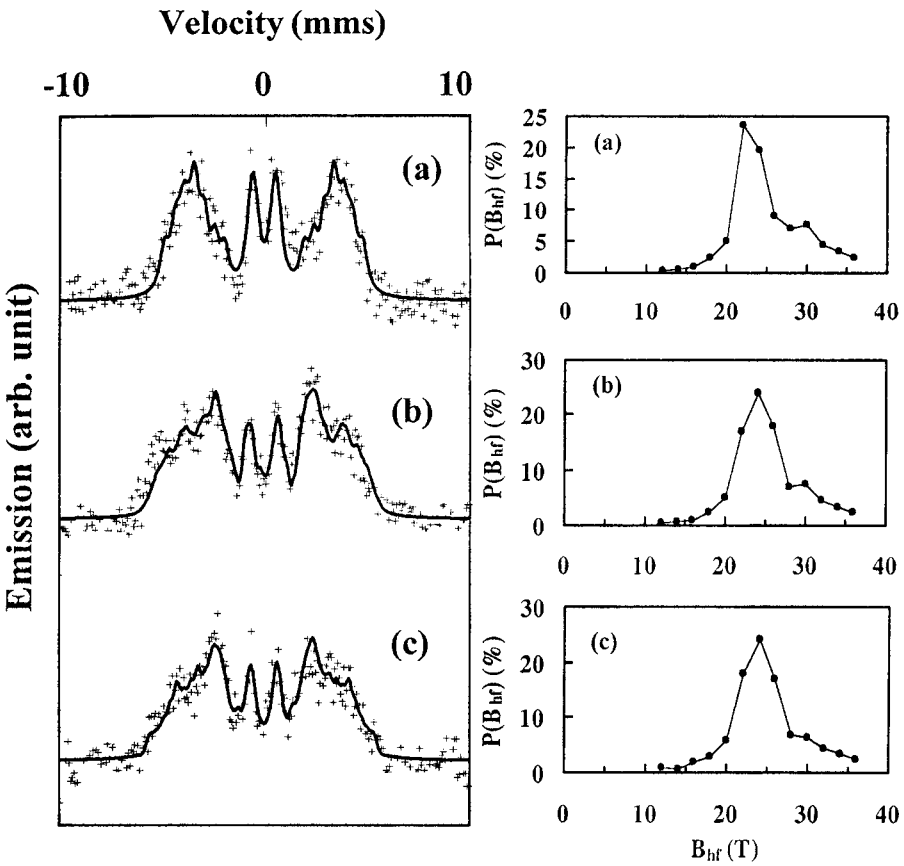

Figure 6. Mössbauer spectra and hyperfine-field distributions of $Tb(Fe_{0.55}Co_{0.45})_{1.5}$ films: (a) film A, (b) C and (c) D.

Table 2. Room-temperature magnetic and magnetostrictive characteristics of the as-deposited $Tb(Fe_{0.55}Co_{0.45})_{1.5}$ films: M_S, $\mu_0 H_{C\parallel}$, $\langle B_{hf}\rangle$, β and λ $(= \lambda_\parallel - \lambda_\perp)$ are the saturation magnetization, film-plane coercive field, average hyperfine field, Fe-spin oriented angle and intrinsic magnetostriction, respectively.

Sample	M_S (kA m^{-1})	$\mu_0 H_{C\parallel}$ (mT)	$\langle B_{hf}\rangle$ (T)	β (°)	λ (10^{-6})
A	320	80	23.5 ± 0.3	12 ± 5	1080
B	305	130	—	—	985
C	285	230	24.5 ± 0.3	78 ± 5	720
D	290	320	24.5 ± 0.3	80 ± 5	670

The fraction of the magnetostrictive alloy (18% of the total spectrum area) is small. As already mentioned above, this reflects that the thickness of the oxidation layer is sufficient thick in annealed films.

We measured two coefficients, $\lambda_\parallel$ and $\lambda_\perp$, which correspond to the applied field, in the film plane, being respectively parallel and perpendicular to the sample length. For the films under investigation, magnetostriction is almost isotropic in the plane. The intrinsic magnetostriction data, $\lambda = \lambda_\parallel - \lambda_\perp$, measured in the applied magnetic field of $\mu_0 H = 0.7$ T are listed in table 2. It is clearly seen that the magnetostriction of a magnitude of 10^{-3} was achieved for films A and B. The parallel magnetostrictive hysteresis loops are shown in figures 7 and 8 for

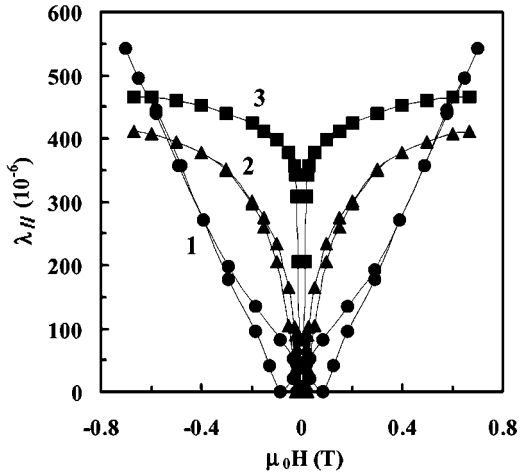

Figure 7. Parallel magnetostrictive hysteresis loops in the external fields for film A: (1) as deposited and (2) annealed at 350 °C and (3) 450 °C.

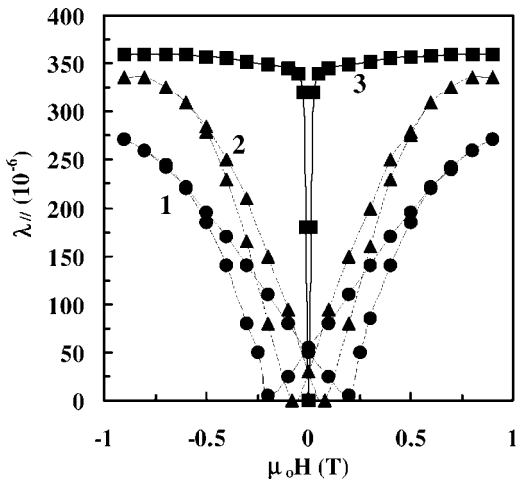

Figure 8. Parallel magnetostrictive hysteresis loops in the external fields for film D: (1) as deposited and (2) annealed at 250 °C and (3) 350 °C.

films A and D, respectively. For the film with perpendicular anisotropy, i.e. the as-deposited sample A, the magnetostriction increases almost linearly in the investigated magnetic field ranges. This implies that it is rather difficult to rotate spins into the film plane. The largest magnetostriction obtained at 0.7 T is $\lambda_{\parallel} = 550 \times 10^{-6}$. The annealing at temperatures between $T_A = 250$ and 450 °C reduces the high-field magnetostriction but enhances the low-field magnetostriction. The optimum annealing is at $T_A = 450$ °C. In this case, the magnetostriction of $\lambda_{\parallel} = 465 \times 10^{-6}$ is saturated at $\mu_0 H = 0.1$ T and $\lambda_{\parallel} = 340 \times 10^{-6}$ is already developed in very low applied magnetic fields of 20 mT. In addition, its coercive field is less than 6 mT. It is worthwhile to mention that in the applied field of 15 mT, the magnetostrictive susceptibility has reached its maximum value, $\chi_\lambda = 1.8 \times 10^{-2}$ T^{-1}. The best magnetostrictive softness is, however, obtained for film D annealed at 350 °C: $\chi_\lambda = 1.8 \times 10^{-2}$ T^{-1} was reached at 10 mT and $\mu_0 H_C$ is below 5 mT (figure 8). We usually associate the field dependence of the

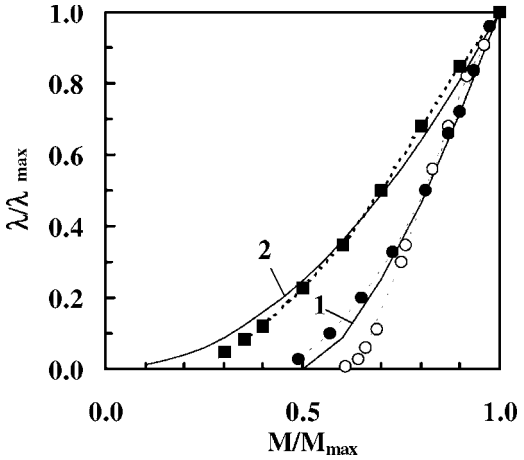

Figure 9. Experimental and theoretical relations between normalized magnetostriction and magnetization for amorphous $Tb(Fe_{0.55}Co_{0.45})_{1.5}$ films. (1) and (2): theoretical curves described for equations (1) and (2), respectively. (■) film A, (●) B and (○) D.

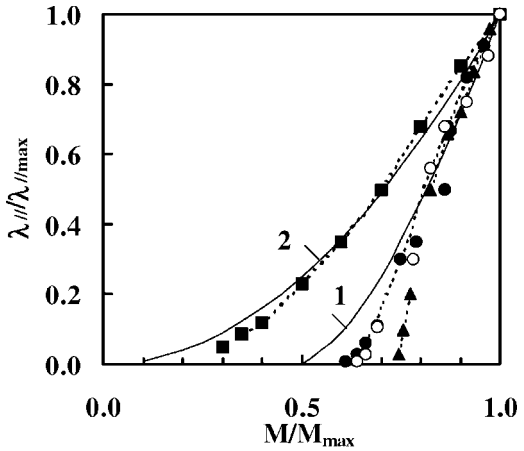

Figure 10. Experimental and theoretical relations between normalized magnetostriction and magnetization for amorphous film A. (1) and (2): theoretical curves described for equations (1) and (2), respectively. (■) as deposited, (●) $T_A = 250\,^{\circ}$C, (▼) 350 °C and (○) 450 °C.

magnetostriction with different types of magnetization processes. For a system of randomly oriented spins and random distribution of the domain walls, the magnetization process takes place in two steps [19]: first, the motion of 180° domain walls leads to a magnetization of M_0 without any contribution to magnetostriction. In the second step, the spins rotate into the direction of the applied magnetic field leading to the change of both magnetization and magnetostriction. For amorphous alloys of randomly three-dimensional spin orientation and of a random distribution of domain walls, M_0 is expected to be $M_{max}/2$. In this case, the relation between magnetostriction and magnetization is given as [20]:

$$\lambda(H)/\lambda_{max} = [2M(H)/M_{max} - 1]^{3/2}. \tag{1}$$

For the rotation of magnetization out of the easy axis to the field direction, the magnetostriction is related to magnetization as follows [19]:

$$\lambda(H)/\lambda_{max} = [M(H)/M_{max}]^2. \tag{2}$$

Taking the values measured in $\mu_0 H = 0.7$ T as λ_{max} and M_{max}, the relation between the normalized magnetostriction and magnetization is presented in figures 9 and 10. For the as-deposited film A with the perpendicular anisotropy, almost no magnetostriction takes place at $M/M_{max} < 0.3$ and the experimental data are close to the curve described by equation (2) (see figure 9). It is possible that, in this film, the magnetization process is governed mainly by the rotation of spins. For the as-deposited films with the parallel anisotropy (i.e. films B and D), the experimental λ/λ_{max} data are rather close to the curve described by equation (1) (see also figure 9). Note that, after annealing at 250, 350 and 450 °C, λ/λ_{max} of the film A starts at an M/M_{max}-value which is even higher than $M_{max}/2$ (see figure 10). In this case, it is possible that the spins are pulled into the plane by the shape anisotropy (i.e. the demagnetizing field) and the randomly in-plane oriented spin structure was formed. This would lead to a magnetization remanence, which is appreciably higher than in the case of the randomly three-dimensional spin orientation.

4. Concluding remarks

In this work, Tb–FeCo films with different magnetic and magnetostrictive behaviours have been studied. An optimization of the magnetostriction at room temperature has been realized by combining not only the rare earth concentration and the substitution of Fe by Co, but also the annealing effects. Excellent magnetic softness is achieved in the films with coercivity $\mu_0 H_C < 5$ mT, saturation field $\mu_0 H_S \approx 20$ mT and, especially, magnetostrictive susceptibility $\chi_\lambda = 1.8 \times 10^{-2}$ T^{-1} obtained at 10 mT. These characteristics make these films useful for applications.

Acknowledgment

This work was funded by the Vietnam National University, Hanoi within the project QG.99.08.

References

[1] Claeyssen F, Lhermet N, Le Letty R and Bouchilloux P 1997 *J. Alloys Compounds* **258** 61
[2] Quandt E 1997 *J. Alloys Compounds* **258** 126
[3] Trémolet de Lacheisserise E, Mackey K, Betz J and Peuzin J C 1998 *J. Alloys Compounds* **275–277** 685
[4] Duc N H *Handbook on the Physics and Chemistry of Rare Earths* vol 28, ed K A Gschneidner Jr and L Eyring (Amsterdam: North-Holland) at press
[5] Fischer S F, Kelsch M and Kronmüller H 1999 *J. Magn. Magn. Mater.* **195** 545
[6] Duc N H, Mackay K, Betz J and Givord D 1996 *J. Appl. Phys.* **79** 973
[7] Duc N H, Mackay K, Betz J and Givord D 2000 *J. Appl. Phys.* **87** 834
[8] Clark A E 1980 *Ferromagnetic Materials* vol 1, ed E P Wohlfarth (Amsterdam: North-Holland) p 531
[9] Quandt E 1994 *J. Appl. Phys.* **75** 5653
[10] Grundy P G, Lord D G and Williams P I 1994 *J. Appl. Phys.* **76** 7003
[11] Danh T M, Duc N H, Thanh H N and Teillet J 2000 *J. Appl. Phys.* **87** 7208
[12] Trémolet de Lacheisserise E and Peuzin J C 1994 *J. Magn. Magn. Mater.* **136** 189
[13] Betz J, du Trémolet de Lacheisserise E and Baczewski L T 1996 *Appl. Phys. Lett.* **68** 132–3
[14] Choi Y S, Lee S R, Han S H, Kim H J and Lim S H 1997 *J. Alloys Compounds* **258** 155
[15] Forkl A, Hirscher M, Mizoguchi T, Kronmüller H and Habermeier H U 1991 *J. Magn. Magn. Mater.* **93** 261
[16] Hernando A, Prados C and Prieto C 1996 *J. Magn. Magn. Mater.* **157/158** 501
[17] Zen D Z, Wang T S, Liu L F, Zai J W and Sha K T 1979 *J. Physique* **40** 243
[18] Wada M, Uchida H and Kaneko H 1997 *J. Alloys Compounds* **258** 169
[19] Chikazumi S 1964 *Physics of Magnetism* (New York: Wiley)
[20] Schatz F, Hirscher M, Schnell M, Flik G and Krönmuller H 1994 *J. Appl. Phys.* **76** 5380